Original Research Communication

NADPH Oxidase-Mediated Triggering of Inflammasome Activation in Mouse Podocytes and Glomeruli during Hyperhomocysteinemia

Justine M. Abais[1], Chun Zhang[1], Min Xia[1], Qinglian Liu[2], Todd W. B. Gehr[3], Krishna M. Boini[1] and Pin-Lan Li[1]

Departments of [1]Pharmacology and Toxicology, [2]Physiology and Biophysics, and [3]Internal Medicine, Medical College of Virginia, Virginia Commonwealth University, Richmond, VA 23298, USA

Running Title: NADPH oxidase and inflammasome activation in podocytes

Address for correspondence:

Pin-Lan Li, MD, PhD
Department of Pharmacology and Toxicology
Virginia Commonwealth University
410 N, 12th Street, Richmond, VA, 23298
Phone: (804) 828 4793
Fax: (804) 828 4794
E-mail: pli@vcu.edu

Word Count: 4238

Number of References: 36

Number of Greyscale Illustrations: 4

Number of Color Illustrations: 4

ABSTRACT

Aim: Our previous studies have shown that NOD-like receptor protein (NALP3) inflammasome activation is importantly involved in podocyte dysfunction and glomerular sclerosis induced by hyperhomocysteinemia (hHcys). The present study was designed to test whether NADPH oxidase-mediated redox signaling contributes to homocysteine (Hcys)-induced activation of NALP3 inflammasomes, an intracellular inflammatory machinery in podocytes *in vitro* and *in vivo*. ***Results****: In vitro* confocal microscopy and size exclusion chromatography revealed that upon NADPH oxidase inhibition by gp91^{phox} siRNA, gp91*ds-tat* peptide, diphenyleneiodonium (DPI) or apocynin, aggregation of inflammasome proteins NALP3, apoptosis-associated speck-like protein (ASC), and caspase-1 was significantly attenuated in mouse podocytes. This NADPH oxidase inhibition also resulted in diminished Hcys-induced inflammasome activation, evidenced by reduced caspase-1 activity and interleukin-1β (IL-1β) production. Similar findings were observed *in vivo* where gp91$^{phox-/-}$ mice and mice receiving a gp91*ds-tat* treatment exhibited markedly reduced inflammasome formation and activation. Furthermore, *in vivo* NADPH oxidase inhibition protected the glomeruli and podocytes from hHcys-induced injury as shown by attenuated proteinuria, albuminuria and glomerular sclerotic changes. This might be attributed to the fact that gp91$^{phox-/-}$ and gp91*ds-tat*-treated mice had abolished infiltration of macrophages and T cells into the glomeruli during hHcys. ***Innovation****:* Our study for the first time links NADPH oxidase to the formation and activation of NALP3 inflammasomes in podocytes. ***Conclusion****:* Hcys-induced NADPH oxidase activation is importantly involved in the switching on of NALP3 inflammasomes within podocytes, which leads to the downstream recruitment of immune cells, ultimately resulting in glomerular injury and sclerosis.

Key words: Homocysteinemia; Inflammasome; NADPH oxidase; Glomerular sclerosis

INTRODUCTION

Hyperhomocysteinemia (hHcys) has been regarded as an important independent risk factor for many degenerative diseases and pathological processes, including end-stage cardiovascular, neurological and renal diseases (1,9,19). Studies from our laboratory and by others have demonstrated that hHcys induces glomerular injury, affecting glomerular endothelial cells, mesangial cells, and podocytes (27-28,34). hHcys also induces glomerular damage by inhibition of extracellular matrix degradation and production of local oxidative stress, contributing to the sclerotic process and eventually leading to the loss of renal function (21,30). Despite extensive studies, the early mechanisms triggering the pathogenic actions of hHcys are not yet fully understood.

More recently, we demonstrated that hHcys may generate its detrimental effects by activation of NALP3-centered inflammasomes, an intracellular inflammatory machinery in podocytes. This proteolytic, high molecular weight complex is primarily comprised of NALP3, the adaptor protein ASC, and caspase-1, where each component is necessary for inflammasome assembly and release of active caspase-1 (16). The activation of these inflammasomes during hHcys turns on local inflammatory response, inducing kidney senescence and progressive degenerative glomerular dysfunction and sclerosis, where active caspase-1 promotes maturation of IL-1β to induce decreases in nephrin expression in podocytes (33). However, it remains to be determined how the NALP3 inflammasomes are formed and activated during hHcys and how this induces glomerular degenerative pathology, ultimately leading to end-stage renal disease.

In this regard, several mechanisms underlying inflammasome activation have been reported including lysosome rupture, ion channel gating, and reactive oxygen species (ROS) activation (23). Activation of the NALP3 inflammasome by increased ROS, the most widely accepted and considered to be the most plausible mechanism, suggests that this inflammasome is a general sensor for changes in cellular oxidative stress. ROS activation of inflammasomes within podocytes may be an early initiating mechanism of glomerular injury during hHcys, because the production of ROS has been considered to be one of the major early factors mediating hHcys-induced glomerular injury (24,31). In the kidney, there are many enzymatic systems that contribute to the production of ROS, including the mitochondria, xanthine/xanthine oxidase, and nicotinamide adenine dinucleotide phosphate (NADPH) oxidase. However, NADPH oxidase has been considered as the major source of superoxide in the kidney, and its action relies on an enzymatic complex with five subunits including $gp91^{phox}$, $p47^{phox}$, $p67^{phox}$, and Rac1/2, all being reported to be expressed in the kidney (6). Furthermore, we have demonstrated the importance of NADPH oxidase in the pathogenesis of hHcys-induced glomerular sclerosis by showing that inhibition of NADPH oxidase and its subunits can attenuate glomerular damage and restore normal renal function (35). Similarly, antioxidants have been shown to ameliorate Hcys-induced toxicity (14). On the other hand, there are reports that hHcys-induced renal injury or other organ damages are also associated with local inflammatory response and corresponding pathological actions (8,20). It is possible that NADPH oxidase activation at the early stage of hHcys triggers the formation of inflammasomes, resulting in a downstream local inflammatory response.

The present study hypothesized that NADPH oxidase-mediated redox signaling may play an essential role in triggering hHcys-induced inflammasome activation within podocytes, thereby inducing glomerular inflammatory injury such as immune cell infiltration and consequently leading to glomerular sclerosis. To test this hypothesis, we first used cultured murine podocytes to examine whether inhibition of NADPH oxidase attenuates Hcys-induced NALP3 inflammasome formation and activation and also addressed the functional relevance of this early inflammatory event. Using pharmacological inhibitors or mice lacking $gp91^{phox}$ gene, we also tested the *in vivo* role of NADPH oxidase activation in hHcys-induced NALP3 inflammasome formation and activation, glomerular inflammatory pathology and glomerular sclerosis compared with wild-type littermates.

RESULTS

Inhibition of NADPH oxidase attenuated Hcys-induced inflammasome formation

As shown in Figure 1A, confocal microscopic analysis demonstrated that Hcys induced the colocalization of inflammasome markers (NALP3 with ASC and NALP3 with caspase-1) in podocytes compared to control cells. Pretreatment of podocytes with NADPH oxidase inhibitors DPI or gp91*ds-tat* peptide significantly abolished the Hcys-induced aggregation of NALP3 with ASC and NALP3 with caspase-1, suggesting blockade of inflammasome formation in these cells. Furthermore, small interfering RNA against ASC and gp91^{phox} also blocked Hcys-induced inflammasome formation. The Pearson correlation coefficient was calculated for each of the groups and summarized in Figure 1B. In addition, co-immunoprecipitation experiments demonstrated that Hcys significantly increased the binding of NALP3 and caspase-1 together with ASC compared to control cells, which is attenuated in the presence of apocynin and gp91*ds-tat* peptide (Supplementary Figure S1). Together, these results suggest that inhibition of NADPH oxidase or silencing ASC gene attenuates Hcys-induced inflammasome formation in podocytes.

Size-exclusion chromatography (SEC) was employed to further determine the role of NADPH oxidase in the process of Hcys-induced inflammasome complex formation. A representative chromatogram is shown in Figure 2A, illustrating the peaks produced from both a standard and typical protein sample when run and separated by the Sepharose 6 column. As depicted in Figure 2B, under control conditions the specific bands for NALP3 and ASC were located in the low molecular weight fractions (18-22). Upon stimulation with Hcys for 24 hours, the NALP3 and ASC bands markedly shifted to high molecular weight fractions (3-7), termed the inflammasome fractions due to complex formation. However, when NADPH oxidase was inhibited in podocytes

by treatment with gp91*ds-tat* or DPI prior to the addition of Hcys, a clear decrease in inflammasome protein complex aggregation was observed in the high-molecular weight fractions. The intensity of these bands were quantified by ImageJ software and summarized in Figure 2C.

Inhibition of NADPH oxidase blocked inflammasome functionality by suppressing caspase-1 activity and IL-1β secretion

We further tested whether inhibition of NADPH oxidase also attenuates Hcys-induced caspase-1 activity and IL-1β production in podocytes. As shown in Figure 3A, the increase in caspase-1 activity caused by Hcys was markedly inhibited by the NADPH inhibitors apocynin, DPI, gp91*ds-tat*, and gp91^{phox} siRNA, implicating an important role for NADPH oxidase in inflammasome activation. ASC siRNA also produced a similar significant decrease in caspase-1 activity. Figure 3B demonstrated that these decreases in caspase-1 activity also resulted in less IL-1β being converted from the pro-inflammatory cytokine form to the active form during the simultaneous treatment of Hcys with either NADPH oxidase or inflammasome inhibitors.

Inhibition of the inflammasome failed to inhibit Hcys-induced superoxide production

To determine whether NADPH oxidase-derived superoxide plays a role in inflammasome activation, superoxide levels were measured in podocytes pretreated with NADPH oxidase or inflammasome inhibitors in the presence of Hcys. As expected, treatment of podocytes with DPI, gp91*ds-tat*, or gp91^{phox} siRNA produced a distinct decrease in superoxide production when compared to Hcys alone (Figure 3C). Additionally apocynin or gp91*ds-tat* peptide also significantly attenuated the Hcys-induced $O_2^{\cdot -}$ production in the plasma membranes of podocytes (Figure 3D). However, ASC siRNA or caspase-1 inhibition could not prevent the Hcys-induced

increase in superoxide. This suggests that NADPH oxidase activation by Hcys and subsequent production of superoxide is upstream of inflammasome activation, given that inhibition of the inflammasome did not affect the levels of NADPH oxidase-derived superoxide.

Attenuation of Hcys-induced podocyte injury by inhibition of NADPH oxidase or inflammasomes

As shown in Figure 4A, immunofluorescent analysis demonstrated that Hcys stimulation increased desmin expression in podocytes compared to untreated cells. Prior treatment with gp91^{phox} siRNA, ASC siRNA, gp91*ds-tat*, apocynin, DPI, or WEHD decreased this Hcys-induced desmin expression in podocytes. Another podocyte marker, podocin, was markedly reduced upon Hcys stimulation in podocytes, and prior treatment with the same inhibitors almost completely attenuated the decrease in podocin expression. Positive cells were counted and summarized in Figure 4B. These results signify the importance of both NADPH oxidase and inflammasome functionality in this injurious process of podocytes when exposed to Hcys. Using rhodamine-phalloidin to stain F-actin, the control condition exhibited well-defined F-actin fibers which run along the longitudinal axis of these podocytes, and as demonstrated by the obvious lack of distinct fibers, Hcys resulted in a significant loss of these longitudinal fibers as they reorganize to the cell border. A classic and specific inducer of podocyte injury, puromycin aminonucleoside (PAN) (12), served as a positive control (Figure 4C). However, inhibition of NADPH oxidase or inflammasomes hindered Hcys-induced decrease and rearrangement of F-actin. These changes in F-actin staining were summarized in Figure 4D.

Blockade of hHcys-induced glomerular inflammasome formation and activation in glomeruli of gp91$^{phox-/-}$ and gp91*ds-tat*-treated mice

To further confirm the role of NADPH activation *in vivo* in experimental hHcys mice, double fluorescent-immunostaining of kidney slides was performed. As shown in Figure 5A, under control condition NALP3, ASC and caspase-1 were expressed at low levels within the glomeruli, and very few colocalizations of these inflammasome molecules could be detected by confocal microscopy. In gp91$^{phox+/+}$ mice, the colocalization of NALP3 with ASC or caspase-1 markedly increased in glomeruli of FF diet-fed hHcys mice. However, the increased colocalization of NALP3 with ASC or caspase-1 was suppressed in glomeruli of hyperhomocysteinemic gp91$^{phox-/-}$ and gp91*ds-tat*-treated mice. The summarized data were shown in Figure 5B and 5C. In addition, using podocin and desmin as podocyte markers we showed that hHcys-induced inflammasome activation in glomeruli was mostly located in podocytes, as demonstrated by the colocalization of podocin with NALP3 or caspase-1 and desmin with NALP3 or caspase-1. This colocalization was substantially blocked in hyperhomocysteinemic gp91$^{phox-/-}$ mice and gp91*ds-tat*-treated mice (Figure 5A and Supplementary Figure S3). The summarized data were shown in Figure 5D and 5E.

Consistent with decreased aggregation of inflammasome components in the glomeruli, hHcys-enhanced caspase-1 activity and IL-1β production were markedly attenuated in glomeruli of gp91$^{phox-/-}$ and gp91*ds-tat*-treated mice (Figure 6A and 6B). In addition, hHcys-induced glomerular superoxide production was significantly attenuated in gp91*ds-tat*-treated and gp91$^{phox-/-}$ mice compared to their wild-type littermates (Figure 6C). The plasma Hcys concentration was similar in gp91$^{phox+/+}$, gp91$^{phox-/-}$ and gp91*ds-tat*-treated mice on the normal

diet. However, the folate-free (FF) diet significantly increased the plasma Hcys concentration in all three groups compared to normal diet fed mice (gp91$^{phox+/+}$ mice: 12.6 ± 2.0 versus 4.1 ± 0.41 μM of control; gp91$^{phox-/-}$ mice: 13.0 ± 1.6 versus 4.0 ± 0.8 μM of control; gp91*ds-tat* mice: 11.6 ± 1.0 versus 5.1 ± 0.41 μM of control).

In vivo inhibition of NADPH oxidase prevented hHcys-induced glomerular inflammation and injury

As shown in Figure 7, immunohistochemical analysis demonstrated that Hcys stimulation induced macrophage (F4/80+) and T-cell (CD43+) infiltration in the glomeruli of hHcys gp91$^{phox+/+}$ mice. However, the glomeruli of gp91$^{phox-/-}$ and gp91*ds-tat*-treated mice had significantly less macrophage and T-cell recruitment when compared to gp91$^{phox+/+}$ mice on the FF diet (Figure 7). The summarized data were shown in Figure 7B and 7D. These results suggest that normal NADPH oxidase gene expression and activity are required for inflammasome activation and consequent inflammatory response, which includes macrophage and T-cell recruitment and aggregation in glomeruli of mice during hHcys.

Next, we tested whether gp91^{phox} contributes to hHcys-induced glomerular injury. As shown in Figure 8, hHcys significantly increased the urinary protein and albumin in gp91$^{phox+/+}$ mice compared to normal diet-fed mice. Mice treated with gp91*ds-tat* and gp91$^{phox-/-}$ mice had significantly attenuated hHcys-enhanced urinary protein and albumin excretion in FF diet-fed mice, but had no effect in normal diet-fed mice (Figure 8A and 8B). Morphological examinations revealed a typical pathological change in glomerular sclerotic damage indicated by capillary collapse, fibrosis, cellular proliferation and mesangial cell expansion in glomeruli of hHcys

gp91$^{phox+/+}$ mice (Figure 8C). The average glomerular damage index was significantly higher in glomeruli of hHcys gp91$^{phox+/+}$ mice compared to normal diet-fed mice. However, in gp91$^{phox-/-}$ or gp91*ds-tat*-treated mice, hHcys-induced glomerular injuries were significantly inhibited (Figure 8D).

DISCUSSION

The primary goal of the present study is to reveal whether NADPH oxidase-mediated redox signaling contributes to Hcys-induced inflammasome formation or activation and consequent glomerular injury. *In vitro* studies using cultured podocytes and an *in vivo* animal model of hHcys demonstrated that NADPH oxidase is necessary for the formation and activation of NALP3 inflammasomes in podocytes upon Hcys stimulation, thereby leading to podocyte dysfunction, glomerular immune cell recruitment, and ultimately glomerular injury and sclerosis. These results for the first time demonstrate Hcys-induced redox activation of podocyte NALP3 inflammasomes as an early mechanism switching on local inflammatory responses in glomeruli.

hHcys has been known to directly cause deleterious effects in the kidney, promoting a vicious cycle responsible for chronic renal disease, where hHcys decreases renal function and leads to further increased plasma Hcys levels due to decreases in Hcys excretion in the kidney (29). In the human condition, a plasma Hcys concentration <10μM is considered to be within the normal range, 10-16 μM is clinically defined as mild hHcys, 16-30 μM as moderate hHcys, 30-100 μM as intermediate hHcys, and >100μM as severe hHcys (29). For mice, it has been extensively studied that similarly to humans, genetic background and strain of the mice plays an important role in the levels of plasma Hcys concentration, along with gender, diet, and parental effects (5). However, our most recent work demonstrated thorough concentration and time dependent studies that in an *in vitro* setting, a 40 μM treatment for 24 hours in cultured podocytes is sufficient to activate an inflammasome-stimulating response, verifying the effect we see *in vivo* (33). Indeed, the present study showed significant glomerular damage observed in gp91$^{phox+/+}$ mice fed a FF diet for 4 weeks. Coinciding with this glomerular damage characterized by our report and others

to include mesangial cell expansion, overall cell proliferation, and capillary collapse (7,35), hHcys caused a significant increase in proteinuria and albuminuria, indicative of an impaired glomerular filtration membrane. In previous studies, these damaging effects of hHcys have been well correlated with its ability to stimulate the inflammatory response. Proinflammatory mediators, like MCP-1, NF-kB, interleukin-8, and adhesion molecules VCAM-1 and E-selectin, have been demonstrated to be upregulated during hHcys (2,25). Furthermore, it has been shown that hHcys results in the recruitment of lymphocytes (18). However, it remains unknown how hHcys or Hcys *in vitro* activates this response of the innate immune system in glomeruli. We have recently reported that Hcys can activate NALP3 inflammasomes in podocytes, an intracellular molecular switch of inflammation (33). Inflammasome activation has also been implicated in a number of inflammatory and metabolic diseases, including obesity, gout, hypersensitivity, silicosis, and diabetes, where inhibition of the inflammasome proteins NALP3, ASC, or caspase-1 significantly attenuates the downstream inflammatory reaction produced under these conditions (3,17,26,36). Similarly, our report showed that inhibition of either ASC or caspase-1 could prevent podocyte and glomerular damage induced by hHcys, improving renal structural and functional integrity (33), suggesting an important role for inflammasome activation in mediating the deleterious effects of hHcys.

The present study further explored the mechanism by which NALP3 inflammasomes are activated in podocytes *in vitro* by Hcys and *in vivo* by experimental hHcys. It has been reported that many endogenous and exogenous danger signals activate the inflammasome, and it has been of great interest as to how all of these very diverse signals can activate the same molecular machinery to turn on inflammation. Of the proposed models of inflammasome activation, the

ROS model provides a unifying link, utilizing the common aspect that all these danger signals produce changes in oxidative stress, making NALP3 a more general sensor detecting these changes in oxidative stress (23). Interestingly, we and others have found the damaging effects of hHcys to be strongly associated with increased local oxidative stress, majorly through NADPH oxidase (4,14,31). With reports of $gp91^{phox}$/Nox2 being the predominant isoform found in podocytes, our laboratory has also demonstrated that this NADPH oxidase isoform and its activity are essential for hHcys to induce glomerular injury, since knockout of the $gp91^{phox}$ gene in mice protected podocytes and glomeruli from hHcys-induced glomerular sclerosis (35). Therefore, we hypothesized that redox signaling associated with NADPH oxidase in podocytes may be critical in triggering NALP3 inflammasome formation and activation upon Hcys stimulation.

To test this hypothesis, we first performed a series of experiments in cultured podocytes. It was found that pharmacological and genetic interventions to inhibit NADPH oxidase resulted in significant attenuation of NALP3 inflammasome formation, as shown by less aggregation of inflammasome molecules detected by confocal microscopy and SEC. Coinciding with the prevention of inflammasome formation, inhibition of NADPH oxidase gene expression or activity also prevented increases in caspase-1 activity as well as IL-1β production, signifying that NADPH oxidase is necessary for NALP3 inflammasome activation in response to Hcys. In contrast, inhibition of NALP3 inflammasome activation by either ASC siRNA or WEHD, a specific caspase-1 inhibitor, did not affect the ability of NADPH oxidase to produce superoxide, strongly indicating that NADPH oxidase-mediated redox signaling is an upstream event that activates NALP3 inflammasome in podocytes. Although there are reports that NALP3

inflammasomes can be activated by ROS in different cells or tissues (11,23,36), to our knowledge, our results for the first time link NADPH oxidase to the formation and activation of these inflammasomes in podocytes, where Hcys-induced NADPH oxidase activation produces superoxide to conduct redox signaling that triggers the formation of NALP3 inflammasomes and production of inflammatory cytokines like IL-1β.

Next, we tested the *in vivo* triggering action of NADPH oxidase activation in the formation of NALP3 inflammasomes using mice lacking $gp91^{phox}$ gene and in mice treated with NADPH oxidase inhibitory peptide, gp91*ds-tat.* Although the strategies used to genetically and pharmacologically inhibit NADPH oxidase in mice were not podocyte-specific, confocal results demonstrated that this inhibition prevented hHcys-induced NALP3 inflammasome formation as shown by less colocalization of NALP3 with ASC and NALP3 with caspase-1, which mainly occurred in podocytes given the increased colocalization of NALP3 molecules with podocin and desmin within glomeruli. Correspondingly, both interventions also inhibited hHcys-induced activation of NALP3 inflammasomes, confirmed by decreased caspase-1 activity and IL-1β production. The inflammatory response in glomeruli during hHcys, indicated by recruitment of macrophages and T-cells, was also significantly suppressed by both genetic and pharmacological inhibition of NADPH oxidase. These results from *in vivo* animal experiments further support the view that NADPH oxidase-mediated redox signaling promotes the formation and activation of NALP3 inflammasomes in podocytes during hHcys. Again, to our knowledge, these findings represent the first *in vivo* experimental evidence that triggering of NALP3 inflammasomes is attributed to NADPH oxidase-mediated redox signaling, which results in local inflammation in glomeruli during hHcys.

We also performed *in vitro* and *in vivo* experiments to address the functional relevance of NADPH oxidase-mediated triggering of NALP3 inflammasomes on Hcys-stimulated podocyte and glomerular injury. Podocytes, the epithelial cells lining the outermost layer of the glomeruli, are essential for proper filtration, and injury to podocytes is indicative of impaired glomerular filtration, in time leading to glomerular sclerosis (13,15). Foot process effacement, considered as the hallmark sign of podocyte injury, is usually accompanied by the destruction of the actin cytoskeleton, increased expression of slit diaphragm molecule and podocyte injury factor desmin, and reduction of the slit diaphragm molecule podocin which is important for cell polarity and survival. In the presence of Hcys, inhibition, gene deletion or silencing of either inflammasome component ASC or NADPH oxidase subunit gp91^{phox} was able to preserve the morphological structure of podocytes by keeping the distinct arrangement of the F-actin fibers intact and was functionally able to maintain podocin expression and prevent desmin expression. *In vivo* studies showed that gp91$^{phox-/-}$ and gp91*ds-tat*-treated mice had less hHcys-induced podocyte injury indicated by the preservation of podocin staining and podocyte number compared to hyperhomocysteinemic gp91$^{phox+/+}$ mice. Although such protection of podocytes observed in *in vivo* experiments may be due to a suppressed inflammatory response (Figure 7), it is interesting to note that in *in vitro* experiments the direct effects of suppressed inflammasome or NADPH oxidase also protect the functional and structural integrity of podocytes, even before a typical inflammatory response is instigated. This non-inflammatory effect or direct action on podocytes has been reported to be associated with IL-1β-induced podocyte dysfunction (22). In addition to the detrimental actions of hHcys-induced inflammatory response, the early effect of activated inflammasome products, like IL-1β, directly on podocytes may also importantly contribute to

podocyte injury. If triggering of such inflammasomes by NADPH oxidase-derived ROS is blocked, both direct and indirect effects of inflammasome activation in the induction of podocytes injury may be blocked, as shown in our results.

Corresponding to protection of podocytes from Hcys-induced injury, inhibition of inflammasome activation by deletion of $gp91^{phox}$ gene or inhibition of NADPH oxidase activity significantly ameliorated hHcys-induced glomerular injury in mice, as shown by improved proteinuria and albuminuria and decreased sclerotic changes in morphology of glomeruli from mice with hHcys. Inhibition of this inflammasome-triggering mechanism not only protects podocytes from injury, but also prevents glomerular sclerosis, which may be due to decreased podocyte injury as well as suppressed local glomerular inflammatory response. This NADPH oxidase-derived ROS may act as redox signaling messengers to activate the inflammasome, which serves as the bridging and amplifying mechanism leading to a robust inflammatory response that eventually progresses to glomerular sclerosis. These findings provide evidence that either targeting the inflammasomes directly or targeting the mechanisms leading to their activation may be an effective therapeutic strategy for the prevention and early treatment of glomerular sclerosis and other end-stage organ damage resulted from hHcys.

In summary, the present study demonstrated that in the very early stages of glomerular damage, Hcys *in vitro* or hHcys *in vivo* stimulated the formation and activation of the NALP3 inflammasome, which initiated early injurious events in podocytes and glomeruli, leading to more serious glomerular injury and ultimate sclerosis. This NALP3 inflammasome activation, podocyte injury, and the glomerular pathology induced by hHcys could be substantially

suppressed by inhibition of NADPH oxidase. These results may establish a new concept that NADPH oxidase-derived ROS upon Hcys stimulation trigger the formation and activation of NALP3 inflammasomes and thereby produce IL-1β and other factors, leading to podocyte and glomerular injury, potentially progressing into glomerular sclerosis.

INNOVATION

hHcys stimulates the formation and activation of a novel intracellular inflammatory machinery, termed the inflammasomes, leading to podocyte injury and eventual glomerular sclerosis. The present study for the first time demonstrates that hHcys-induced activation of inflammasomes in podocytes is attributed to NADPH oxidase-mediated redox signaling, where the production of ROS may not only be involved in inflammation-induced tissue injury by oxidative damage, but may also serve as signaling molecules to regulate this very early activation of the inflammasomes.

MATERIALS AND METHODS

Animals

Eight-week old, male gp91$^{phox+/+}$ and gp91$^{phox-/-}$ mice (Jackson Laboratories, Bar Harbor, ME, USA) were uninephrectomized to accelerate renal injury, as described previously (32). After allowing a week for recovery after surgery, gp91$^{phox+/+}$ and gp91$^{phox-/-}$ mice were fed either a normal diet or a folate-free (FF) diet for 4 weeks to induce hHcys (34). Another group of gp91$^{phox+/+}$ mice were injected intraperitoneally with gp91*ds-tat* or scrambled gp91*ds-tat* at a dose of 5 mg/kg every day, while being maintained on the FF diet for 4 weeks (10). This custom gp91*ds-tat* peptide constructed with a *tat* sequence to enable cell membrane penetration and inhibition of NADPH oxidase, was synthesized by RS Synthesis (Louisville, KY) with the following amino acid sequence: YGRKKRRQRRRCSTRIRRQL. gp91$^{phox+/+}$, gp91$^{phox-/-}$, and gp91*ds-tat* mice were placed in metabolic cages and urine samples were collected for 24 hours before collecting blood samples, sacrificing, and harvesting tissues for analysis. All protocols were approved by the Institutional Animal Care and Use Committee of Virginia Commonwealth University.

Confocal microscopic detection of inflammasome proteins

Indirect immunofluorescent staining was used to determine the colocalization of inflammasome proteins in both podocytes and in glomeruli of the mouse kidney. Detailed double immunofluorescent staining detection methods are presented in the online supplementary materials.

Size-exclusion chromatography: SEC was performed in podocytes as described previously (33). The detailed SEC method was presented in the online supplementary materials.

All other methods are described in the online supplementary materials.

ACKNOWLEDGMENTS

This work was supported by grants DK54927, HL075316, and HL57244 (to P.L.) and 1F31AG043289-01 (to J.M.A.) from the National Institutes of Health.

AUTHOR DISCLOSURE STATEMENT

No competing financial interests exist.

LIST OF ABBREVIATIONS

APO: apocynin; **ASC**: apoptosis associated speck-like protein; **ASCsi**: ASC siRNA; **Ctrl**: Control; **DPI**: diphenyleneiodonium; **FF**: folate-free diet; **gp91pep**: gp91*ds-tat*; **gp91si**: gp91^{phox} siRNA; **Hcys**: homocysteine; **hHcys**: hyperhomocysteinemia; **IL-1β**: interleukin-1β; **NALP3**: NOD-like receptor protein; **ND**: Normal Diet; **PAN**: puromycin aminonucleoside; **ROS**: reactive oxygen species; **Scram**: Scramble siRNA; **SEC:** size-exclusion chromatography; **Vehl**: Vehicle.

REFERENCES

1. Cavalca V, Cighetti G, Bamonti F, Loaldi A, Bortone L, Novembrino C, De Franceschi M, Belardinelli R, Guazzi MD. Oxidative stress and homocysteine in coronary artery disease. *Clin Chem* 47: 887-92, 2001.

2. Dai J, Wang X. Immunoregulatory effects of homocysteine on cardiovascular diseases. *Sheng Li Xue Bao* 59: 585-92, 2007.

3. Dostert C, Petrilli V, Van Bruggen R, Steele C, Mossman BT, Tschopp J. Innate immune activation through Nalp3 inflammasome sensing of asbestos and silica. *Science* 320: 674-7, 2008.

4. Edirimanne VE, Woo CW, Siow YL, Pierce GN, Xie JY, O K. Homocysteine stimulates NADPH oxidase-mediated superoxide production leading to endothelial dysfunction in rats. *Can J Physiol Pharmacol* 85: 1236-47, 2007.

5. Ernest S, Hosack A, O'Brien WE, Rosenblatt DS, Nadeau JH. Homocysteine levels in A/J and C57BL/6J mice: genetic, diet, gender, and parental effects. *Physiol Genomics* 21: 404-10, 2005.

6. Gill PS, Wilcox CS. NADPH oxidases in the kidney. *Antioxid Redox Signal* 8: 1597-607, 2006.

7. Henegar JR, Bigler SA, Henegar LK, Tyagi SC, Hall JE. Functional and structural changes in the kidney in the early stages of obesity. *J Am Soc Nephrol* 12: 1211-7, 2001.

8. Hofmann MA, Lalla E, Lu Y, Gleason MR, Wolf BM, Tanji N, Ferran LJ, Jr., Kohl B, Rao V, Kisiel W, Stern DM, Schmidt AM. Hyperhomocysteinemia enhances vascular inflammation and accelerates atherosclerosis in a murine model. *J Clin Invest* 107: 675-83, 2001.

9. Ientile R, Curro M, Ferlazzo N, Condello S, Caccamo D, Pisani F. Homocysteine, vitamin determinants and neurological diseases. *Front Biosci (Schol Ed)* 2: 359-72, 2010.

10. Jackson EK, Gillespie DG, Zhu C, Ren J, Zacharia LC, Mi Z. Alpha2-adrenoceptors enhance angiotensin II-induced renal vasoconstriction: role for NADPH oxidase and RhoA. *Hypertension* 51: 719-26, 2008.

11. Jin C, Flavell RA. Inflammasome activation. The missing link: how the inflammasome senses oxidative stress. *Immunol Cell Biol* 88: 510-2, 2010.

12. Koshikawa M, Mukoyama M, Mori K, Suganami T, Sawai K, Yoshioka T, Nagae T, Yokoi H, Kawachi H, Shimizu F, Sugawara A, Nakao K. Role of p38 mitogen-activated protein kinase activation in podocyte injury and proteinuria in experimental nephrotic syndrome. *J Am Soc Nephrol* 16: 2690-701, 2005.

13. Kriz W. Podocyte is the major culprit accounting for the progression of chronic renal disease. *Microsc Res Tech* 57: 189-95, 2002.

14. Malinowska J, Olas B. Effect of resveratrol on hemostatic properties of human fibrinogen and plasma during model of hyperhomocysteinemia. *Thromb Res* 126: e379-82, 2010.

15. Marshall CB, Pippin JW, Krofft RD, Shankland SJ. Puromycin aminonucleoside induces oxidant-dependent DNA damage in podocytes in vitro and in vivo. *Kidney Int* 70: 1962-73, 2006.

16. Martinon F, Mayor A, Tschopp J. The inflammasomes: guardians of the body. *Annu Rev Immunol* 27: 229-65, 2009.

17. Martinon F, Petrilli V, Mayor A, Tardivel A, Tschopp J. Gout-associated uric acid crystals activate the NALP3 inflammasome. *Nature* 440: 237-41, 2006.

18. Postea O, Koenen RR, Hristov M, Weber C, Ludwig A. Homocysteine up-regulates vascular transmembrane chemokine CXCL16 and induces CXCR6+ lymphocyte recruitment in vitro and in vivo. *J Cell Mol Med* 12: 1700-9, 2008.

19. Robinson K, Gupta A, Dennis V, Arheart K, Chaudhary D, Green R, Vigo P, Mayer EL, Selhub J, Kutner M, Jacobsen DW. Hyperhomocysteinemia confers an independent increased risk of atherosclerosis in end-stage renal disease and is closely linked to plasma folate and pyridoxine concentrations. *Circulation* 94: 2743-8, 1996.

20. Sen U, Givvimani S, Abe OA, Lederer ED, Tyagi SC. Cystathionine beta-synthase and cystathionine gamma-lyase double gene transfer ameliorate homocysteine-mediated mesangial inflammation through hydrogen sulfide generation. *Am J Physiol Cell Physiol* 300: C155-63, 2011.

21. Steed MM, Tyagi N, Sen U, Schuschke DA, Joshua IG, Tyagi SC. Functional consequences of the collagen/elastin switch in vascular remodeling in hyperhomocysteinemic wild-type, eNOS-/-, and iNOS-/- mice. *Am J Physiol Lung Cell Mol Physiol* 299: L301-11, 2010.

22. Takano Y, Yamauchi K, Hayakawa K, Hiramatsu N, Kasai A, Okamura M, Yokouchi M, Shitamura A, Yao J, Kitamura M. Transcriptional suppression of nephrin in podocytes by macrophages: roles of inflammatory cytokines and involvement of the PI3K/Akt pathway. *FEBS Lett* 581: 421-6, 2007.

23. Tschopp J, Schroder K. NLRP3 inflammasome activation: The convergence of multiple signalling pathways on ROS production? *Nat Rev Immunol* 10: 210-5, 2010.

24. Ventura E, Durant R, Jaussent A, Picot MC, Morena M, Badiou S, Dupuy AM, Jeandel C, Cristol JP. Homocysteine and inflammation as main determinants of oxidative stress in the elderly. *Free Radic Biol Med* 46: 737-44, 2009.

25. Wang G, Woo CW, Sung FL, Siow YL, O K. Increased monocyte adhesion to aortic endothelium in rats with hyperhomocysteinemia: role of chemokine and adhesion molecules. *Arterioscler Thromb Vasc Biol* 22: 1777-83, 2002.

26. Watanabe H, Gaide O, Petrilli V, Martinon F, Contassot E, Roques S, Kummer JA, Tschopp J, French LE. Activation of the IL-1beta-processing inflammasome is involved in contact hypersensitivity. *J Invest Dermatol* 127: 1956-63, 2007.

27. Yi F, Chen QZ, Jin S, Li PL. Mechanism of homocysteine-induced Rac1/NADPH oxidase activation in mesangial cells: role of guanine nucleotide exchange factor Vav2. *Cell Physiol Biochem* 20: 909-18, 2007.

28. Yi F, Jin S, Zhang F, Xia M, Bao JX, Hu J, Poklis JL, Li PL. Formation of lipid raft redox signalling platforms in glomerular endothelial cells: an early event of homocysteine-induced glomerular injury. *J Cell Mol Med* 13: 3303-14, 2009.

29. Yi F, Li PL. Mechanisms of homocysteine-induced glomerular injury and sclerosis. *Am J Nephrol* 28: 254-64, 2008.

30. Yi F, Xia M, Li N, Zhang C, Tang L, Li PL. Contribution of guanine nucleotide exchange factor Vav2 to hyperhomocysteinemic glomerulosclerosis in rats. *Hypertension* 53: 90-6, 2009.

31. Yi F, Zhang AY, Janscha JL, Li PL, Zou AP. Homocysteine activates NADH/NADPH oxidase through ceramide-stimulated Rac GTPase activity in rat mesangial cells. *Kidney Int* 66: 1977-87, 2004.

32. Yi F, Zhang AY, Li N, Muh RW, Fillet M, Renert AF, Li PL. Inhibition of ceramide-redox signaling pathway blocks glomerular injury in hyperhomocysteinemic rats. *Kidney Int* 70: 88-96, 2006.

33. Zhang C, Boini KM, Xia M, Abais JM, Li X, Liu Q, Li PL. Activation of Nod-like receptor protein 3 inflammasomes turns on podocyte injury and glomerular sclerosis in hyperhomocysteinemia. *Hypertension* 60: 154-62, 2012.

34. Zhang C, Hu JJ, Xia M, Boini KM, Brimson C, Li PL. Redox signaling via lipid raft clustering in homocysteine-induced injury of podocytes. *Biochim Biophys Acta* 1803: 482-91, 2010.

35. Zhang C, Hu JJ, Xia M, Boini KM, Brimson CA, Laperle LA, Li PL. Protection of podocytes from hyperhomocysteinemia-induced injury by deletion of the gp91phox gene. *Free Radic Biol Med* 48: 1109-17, 2010.

36. Zhou R, Tardivel A, Thorens B, Choi I, Tschopp J. Thioredoxin-interacting protein links oxidative stress to inflammasome activation. *Nat Immunol* 11: 136-40, 2010.

FIGURE LEGENDS

Figure 1. NADPH oxidase inhibition attenuates inflammasome formation induced by hHcys in podocytes. A. Confocal images representing the colocalization of NALP3 (green) with ASC (red) and NALP3 (green) with caspase-1 (red) in podocytes. B. Summarized data showing the fold change of PCC for the colocalization of NALP3 with ASC and NALP3 with caspase-1. (n=6-7). Ctrl: Control; Vehl: Vehicle; gp91pep: gp91*ds-tat*; DPI: diphenyleneiodonium; Scram: Scramble siRNA; ASCsi: ASC siRNA; gp91si: $gp91^{phox}$ siRNA. * $P<0.05$ vs. Control; # $P<0.05$ vs. Hcys.

Figure 2. Distribution of inflammasome components after size-exclusion chromatography of podocytes. A. Elution profile of proteins from both a standard and podocyte samples at an absorbance of 280 nm. Molecular mass of the samples were determined by comparison to a gel filtration standard. B. Western blot analysis of protein fractions obtained from untreated, Hcys-treated, and gp91*ds-tat*-treated podocytes probed with anti-NALP3 and ASC antibodies. C. Summarized data showing the band intensities measured from the inflammasome complex fractions (fractions 3-7) of NALP3 and ASC (n=4-6). Ctrl: Control; Vehl: Vehicle; gp91pep: gp91*ds-tat*; DPI: diphenyleneiodonium; gp91sh: $gp91^{phox}$ shRNA, APO: apocynin. * $P<0.05$ vs. Control; # $P<0.05$ vs. Hcys.

Figure 3. Effects of NADPH oxidase inhibition and ASC silencing on Hcys-induced Caspase-1 activity, IL-1β secretion, and superoxide production in podocytes. A. Caspase-1 activity in groups treated with Hcys in the presence of various genetic and pharmacologic inhibitors of NADPH oxidase and the inflammasome (n=6). B. IL-1β production in podocytes

treated with Hcys in the presence of various genetic and pharmacologic inhibitors of NADPH oxidase and the inflammasome (n=6). C. Hcys-induced $O_2^{\cdot-}$ production decreased with treatment of NADPH oxidase inhibitors, but not genetic or pharmacologic inhibitors of the inflammasome (n=5). D. Hcys induced superoxide production in microsomes isolated from cultured podocytes, which was prevented by pharmacological NADPH oxidase inhibitors APO and gp91pep (n=4-5). Ctrl: Control; Vehl: Vehicle; gp91pep: gp91*ds-tat*; DPI: diphenyleneiodonium; Scram: Scramble siRNA; ASCsi: ASC siRNA; gp91si: gp91^{phox} siRNA; APO: apocynin. * P<0.05 vs. Control; # P<0.05 vs. Hcys.

Figure 4. Amelioration of Hcys-induced podocyte dysfunction by NADPH oxidase and inflammasome inhibitors. A. Immunofluorescence staining showed that inhibition of NADPH oxidase activation by gp91^{phox} siRNA, gp91*ds-tat*, apocynin and DPI, or inflammasome inhibition by ASC siRNA or WEHD rescued Hcys-induced expression of podocyte marker podocin (original magnification, x400). Inhibition of NADPH oxidase or inflammasome activation also resulted in suppressed expression of podocyte injury marker desmin. B. Summarized data shows the percentage of podocyte cells positive for podocin and desmin. C. Microscopic images of F-actin by rhodamine-phalloidin staining (original magnification, x400). PAN treatment served as a positive control. D. Summarized data from counting the cells with distinct, longitudinal F-actin fibers. Scoring was determined from 100 podocyte cells on each slide (n=5-6). Ctrl: Control; Vehl: Vehicle; gp91pep: gp91*ds-tat*; DPI: diphenyleneiodonium; Scram: Scramble siRNA; ASCsi: ASC siRNA; gp91si: gp91^{phox} siRNA. * P<0.05 vs. Control; # P<0.05 vs. Hcys.

Figure 5. Attenuation of Hcys-induced inflammasome activation in the glomeruli of gp91$^{phox-/-}$ and gp91*ds-tat*-treated mice on a FF diet. A. Colocalization of NALP3 (green) with ASC (red), NALP3 (green) with caspase-1 (red), and NALP3 (green) with podocyte marker podocin (red) in the mouse glomeruli of gp91$^{phox+/+}$, gp91*ds-tat*, and gp91$^{phox-/-}$ mice fed a normal or FF diet. B and C. Summarized data showing the correlation coefficient between NALP3 with ASC and NALP3 with caspase-1 (n=7). D and E. Summarized data showing the correlation coefficient between NALP3 with podocin and caspase-1 with podocin (n=4-5). *P<0.05 vs. gp91$^{phox+/+}$ on Normal Diet; # P<0.05 vs. gp91$^{phox+/+}$ on FF Diet.

Figure 6. *In vivo* effect of NADPH oxidase inhibition on Hcys-induced caspase-1 activity, IL-1β secretion, and superoxide production. A. Caspase-1 activity in gp91$^{phox+/+}$, gp91*ds-tat*, and gp91$^{phox-/-}$ mice with hHcys induced by the FF diet (n=6). B. IL-1β production induced by hHcys was inhibited in both the mice treated with gp91*ds-tat* and in gp91$^{phox-/-}$ mice (n=6). C. Hcys-induced superoxide production was attenuated in the gp91*ds-tat* and gp91$^{phox-/-}$ groups (n=5). * P<0.05 vs. gp91$^{phox+/+}$ on Normal Diet; # P<0.05 vs. gp91$^{phox+/+}$ on FF Diet.

Figure 7. Inhibition of NADPH oxidase expression and activity prevented hHcys-induced infiltration of macrophages and T-cells into the glomeruli. A. gp91*ds-tat* and gp91$^{phox-/-}$ mice prevented the increased expression and staining of macrophage marker F4/80 that is seen in gp91$^{phox+/+}$ on FF Diet. B. Summarized counts of F4/80 positive glomeruli (n=6). C. gp91*ds-tat* and gp91$^{phox-/-}$ mice prevented the increased expression and staining of T-cell marker CD43 that is seen in gp91$^{phox+/+}$ on FF Diet. D. Summarized counts of CD43 positive glomeruli (n=6). * P<0.05 vs. gp91$^{phox+/+}$ on Normal Diet; # P<0.05 vs. gp91$^{phox+/+}$ on FF Diet.

Figure 8. Inhibition of NADPH oxidase expression and activity protected glomerular function from hHcys-induced injury. A. Hyperhomocysteinemic gp91$^{phox+/+}$ mice produced proteinuria, which was alleviated in the gp91$^{phox-/-}$ or in the gp91*ds-tat*-treated mice (n=6). B. Hyperhomocysteinemic gp91$^{phox+/+}$ mice produced albuminuria, where blockade of NADPH oxidase in gp91$^{phox-/-}$ mice or in gp91*ds-tat*-treated mice prevented this glomerular damage (n=6). C. Glomerular morphological examination by PAS staining demonstrated that gp91*ds-tat* administration or gp91$^{phox-/-}$ mice prevented capillary collapse, fibrosis, cellular proliferation and expansion induced by hHcys (n=4-6). D. Glomerular damage index (GDI) was assessed by a standard semiquantitative analysis to determine severity of glomerular sclerosis. * P<0.05 vs. gp91$^{phox+/+}$ on Normal Diet; # P<0.05 vs. gp91$^{phox+/+}$ on FF Diet.

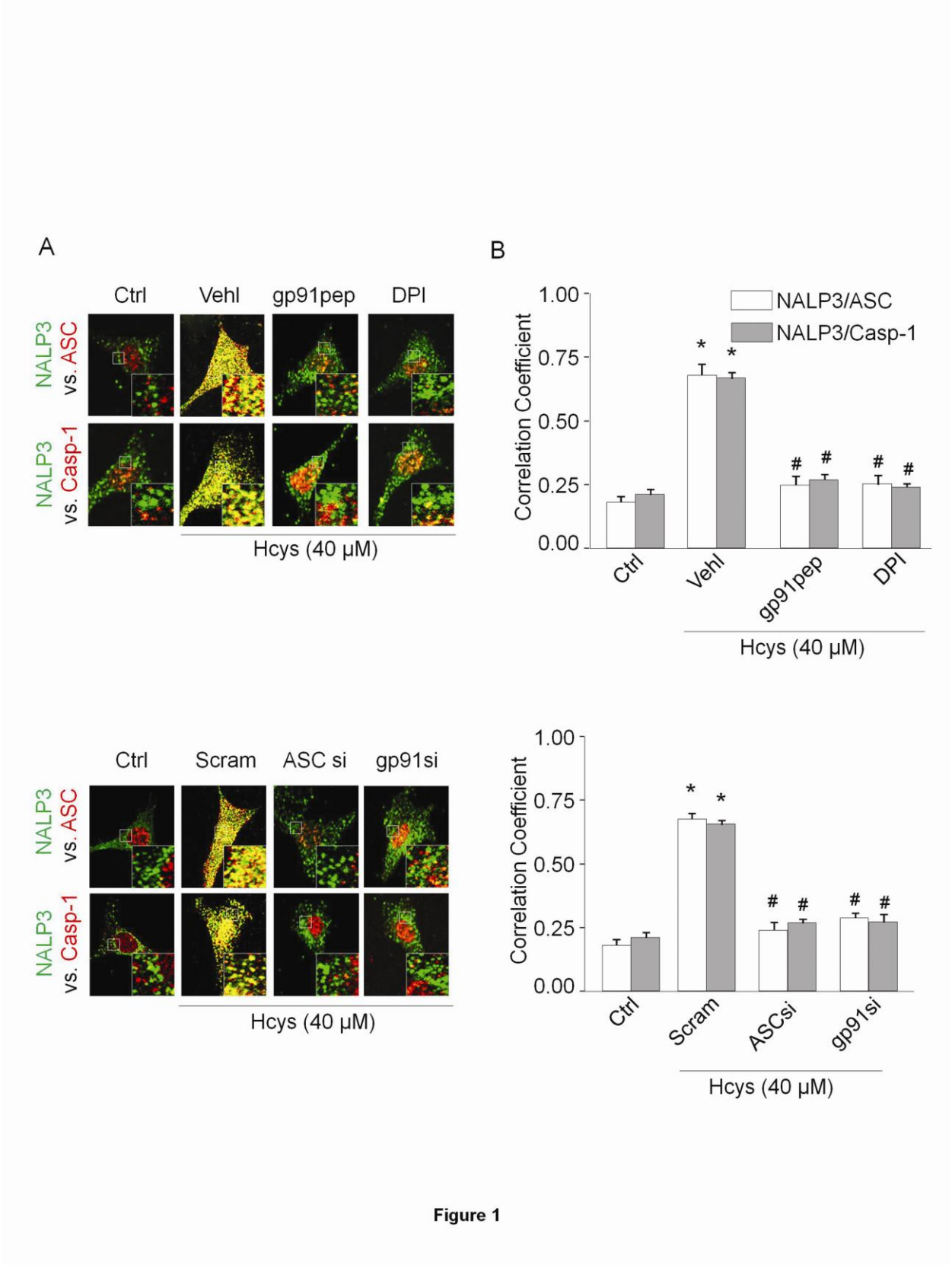

Figure 1

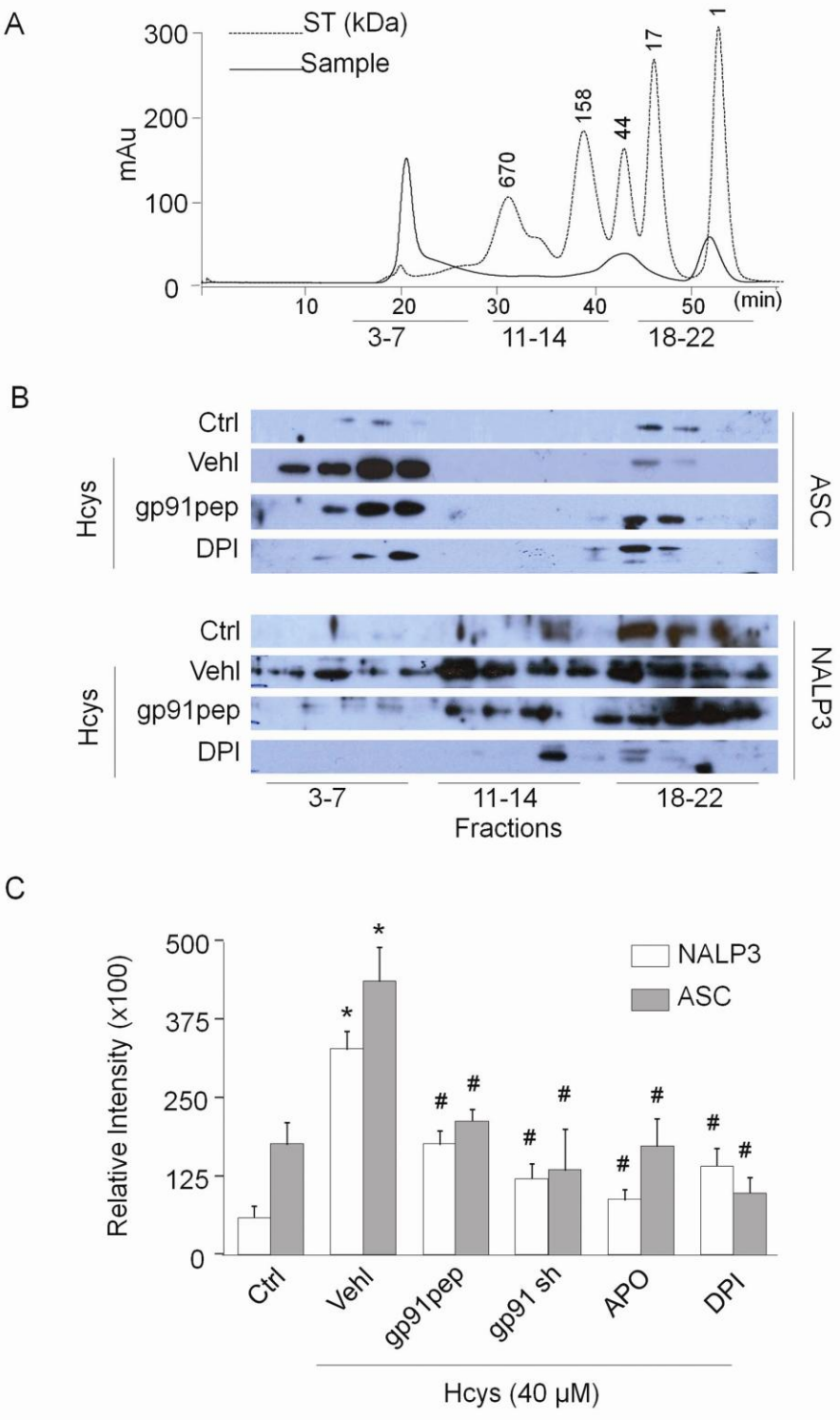

Figure 2

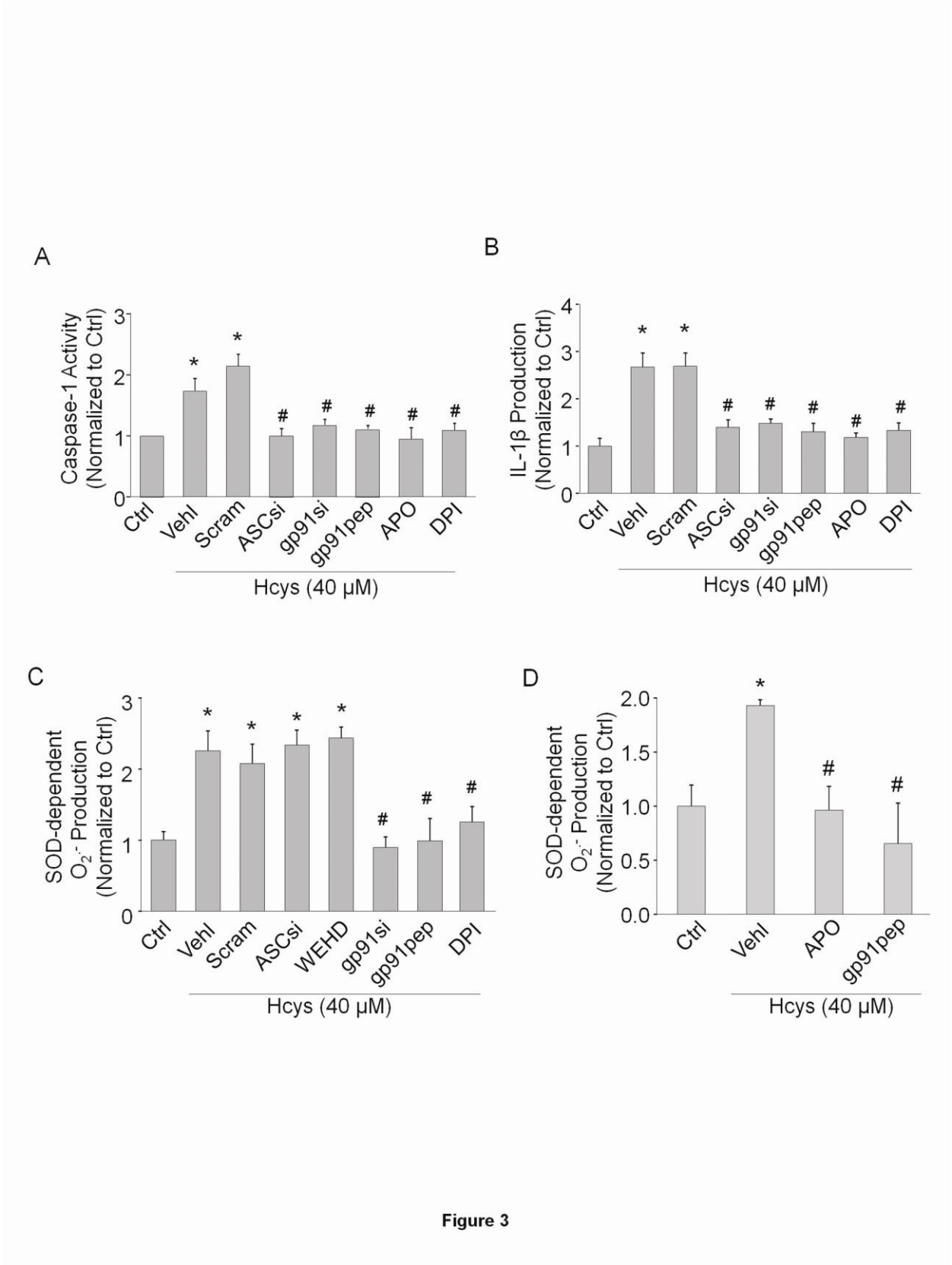

Figure 3

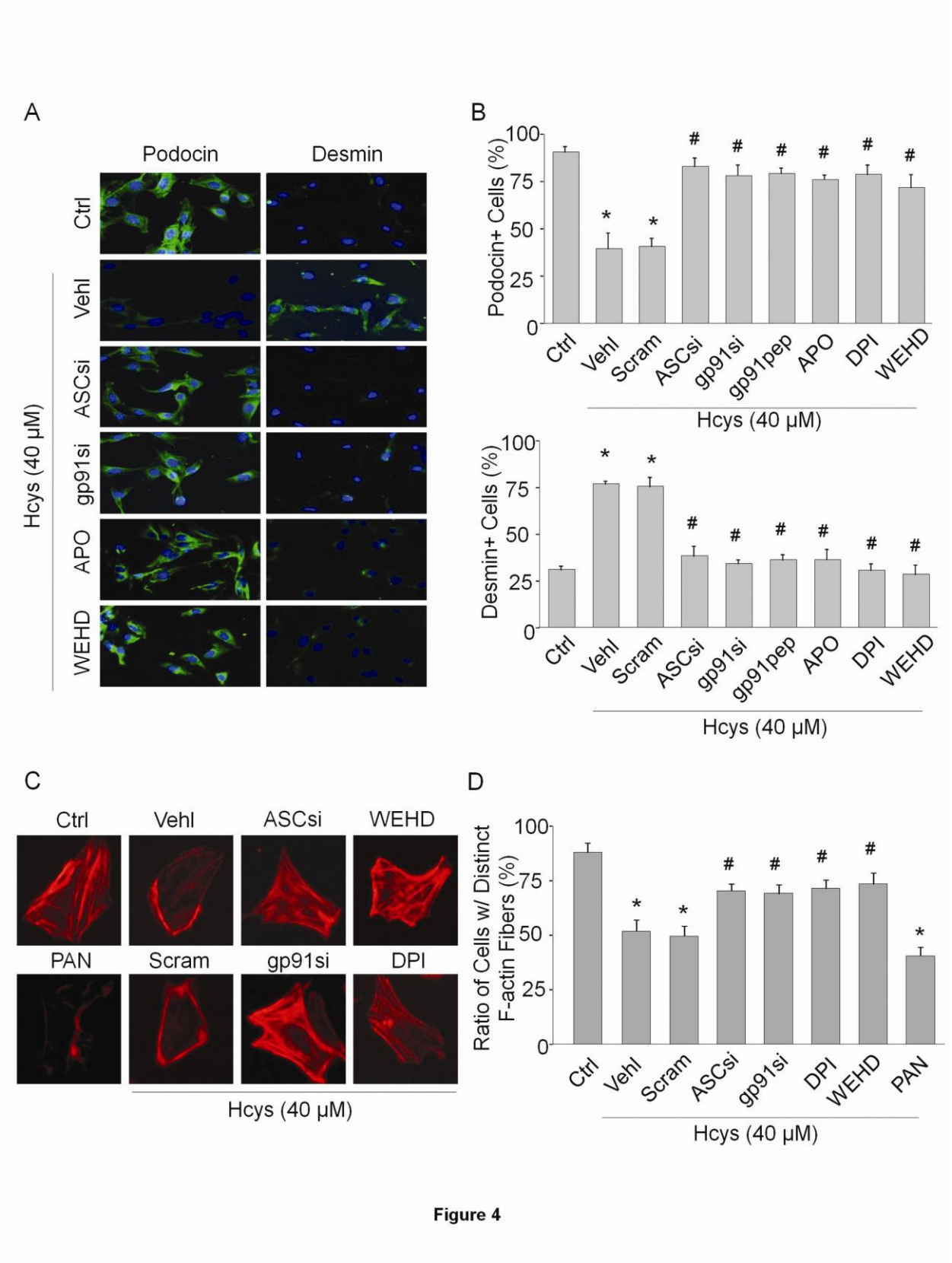

Figure 4

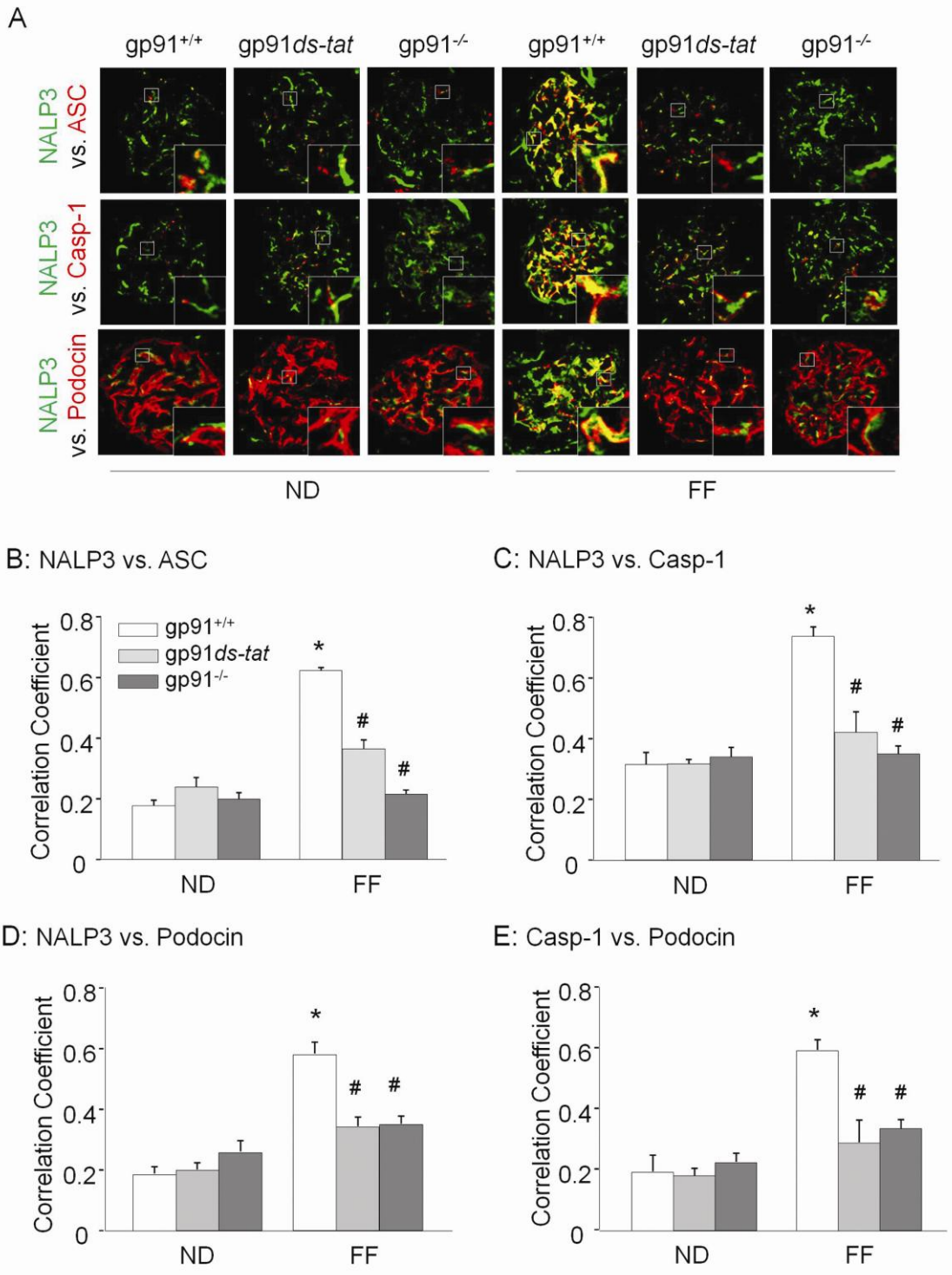

Figure 5

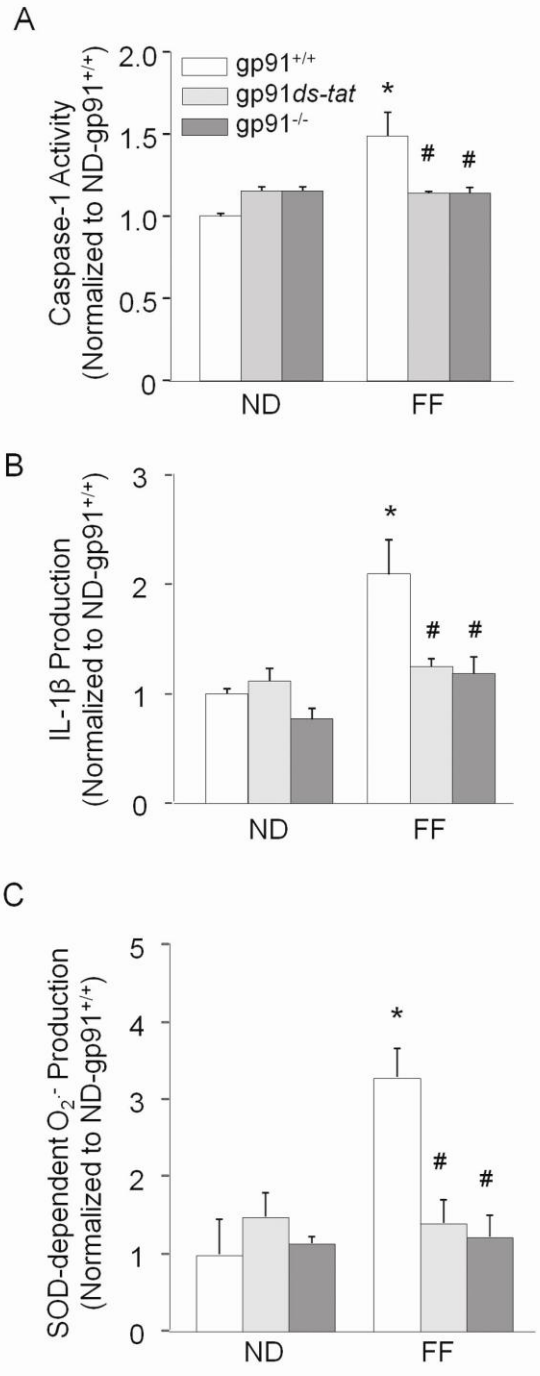

Figure 6

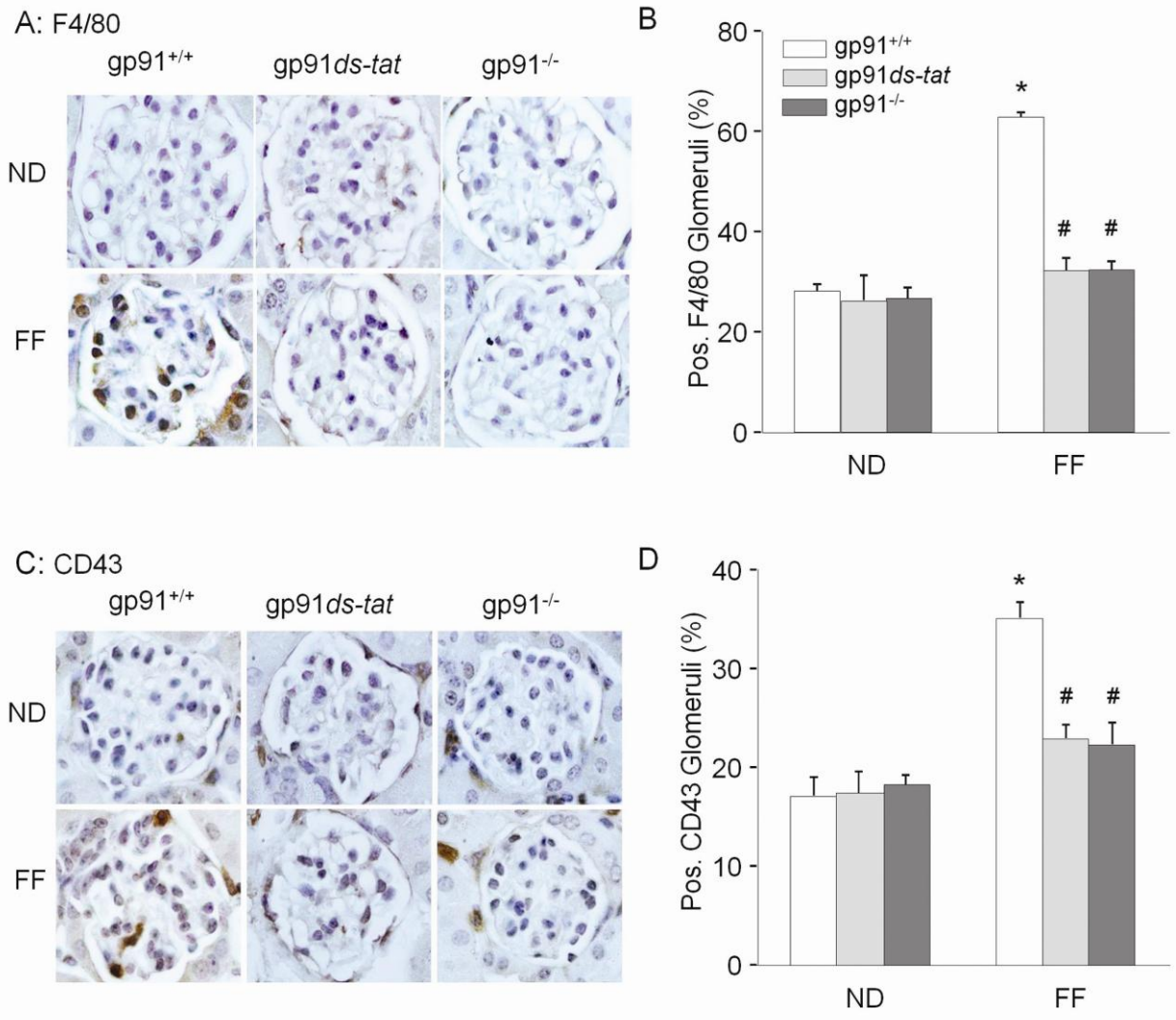

Figure 7

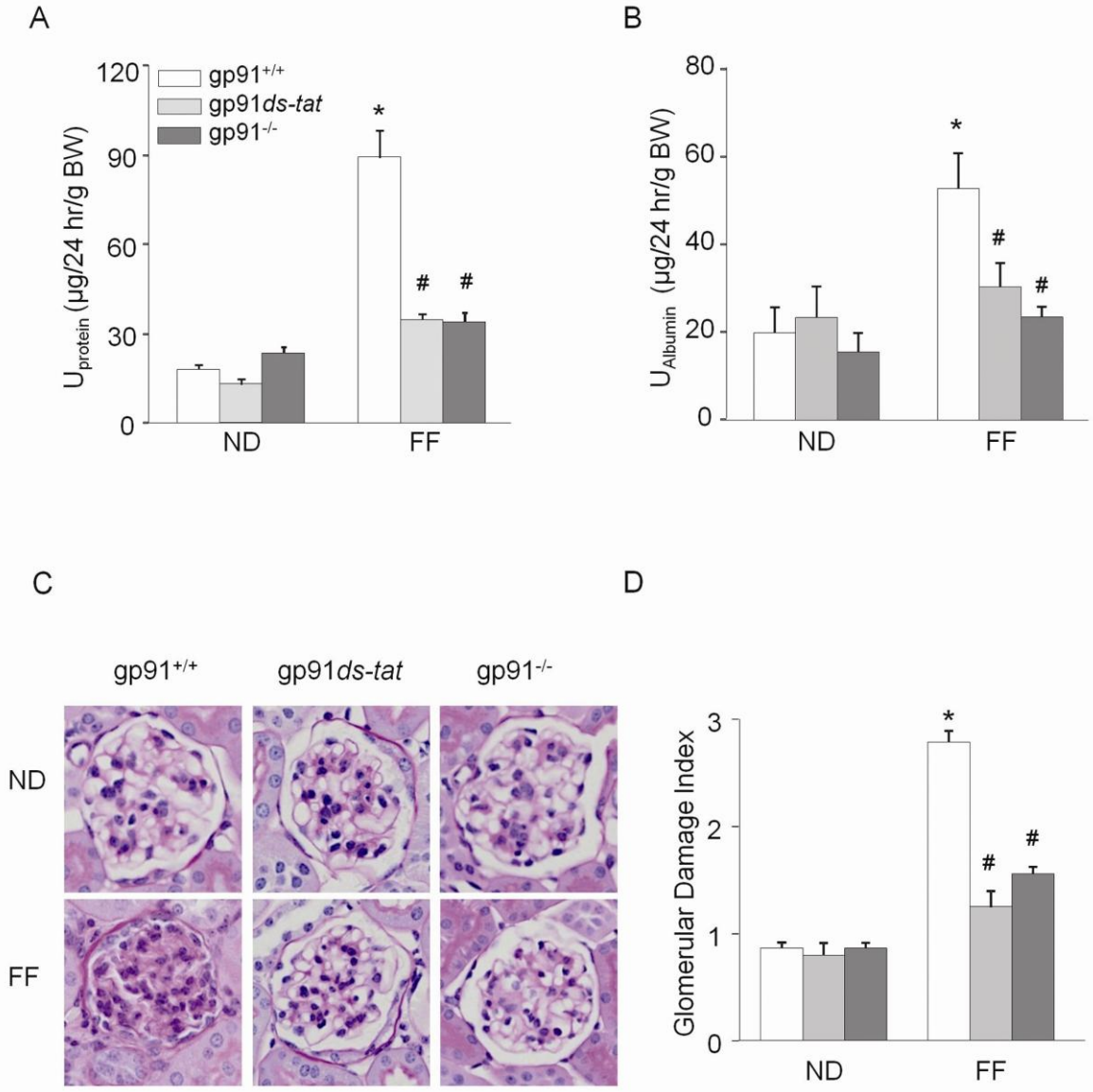

Figure 8

NADPH Oxidase-Mediated Triggering of Inflammasome Activation in Mouse Podocytes and Glomeruli during Hyperhomocysteinemia

Justine M. Abais[1], Chun Zhang[1], Min Xia[1], Qinglian Liu[2], Todd W. B. Gehr[3], Krishna M. Boini[1] and Pin-Lan Li[1]

Departments of [1]Pharmacology and Toxicology, [2]Physiology and Biophysics, and [3]Internal Medicine, Medical College of Virginia, Virginia Commonwealth University, Richmond, VA 23298, USA

ONLINE SUPPLEMENTARY MATERIALS

MATERIALS AND METHODS

Cell culture

A conditionally immortalized mouse podocyte cell line, graciously provided by Dr. Paul E. Klotman (Division of Nephrology, Department of Medicine, Mount Sinai School of Medicine, New York, USA), was constructed with a temperature-sensitive variant of the simian virus (SV40) containing a large T antigen (tsA58) inducible by interferon-γ at 33°C, allowing for cellular proliferation. These cells were cultured and maintained on collagen-coated flasks in RPMI 1640 medium supplemented with 10% fetal bovine serum, 10 U/ml recombinant mouse interferon-γ, 100 U/ml penicillin and 100 mg/ml streptomycin. The podocytes were then passaged and allowed to differentiate at 37℃ for two weeks without interferon-γ before use in

the experiments stated below. Podocytes were treated with L-Hcys, which is considered to be the pathogenic form of Hcys, at a concentration of 40 μM for 24 hours, a dose and treatment time chosen based on previous studies (5).

Confocal microscopic detection of inflammasome proteins

Indirect immunofluorescent staining was used to determine colocalization of the inflammasome proteins in both podocytes and in glomeruli of the mouse kidney. For the colocalization in podocytes, cells were seeded on poly-L-lysine-coated chambers and pre-treated with various NADPH oxidase and inflammasome inhibitors before incubation with 40 μM L-Hcys for 24 hours. Pharmacological NADPH oxidase inhibitors apocynin (100 μM), diphenyleneiodonium (10 μM), and gp91*ds-tat* peptide (5 μM) were added to the cells 1 hour prior to Hcys treatment. Cells were fixed with 4% PFA for 15 minutes, washed with PBS, blocked with 1% BSA in PBS, and incubated overnight at 4 ℃ with the following primary antibodies: goat anti-NALP3 (1:200; Abcam, Cambridge, MA) with rabbit anti-ASC (1:50; Enzo, Plymouth Meeting, PA), or goat anti-NALP3 (1:200) with mouse anti-caspase-1 (1:100; Abcam, Cambridge, MA). For the colocalization in the mouse glomeruli, frozen slides were fixed in acetone then incubated overnight at 4 ℃ with goat anti-NALP3 (1:200) and rabbit anti-ASC (1:50), or goat anti-NALP3 (1:200) and mouse anti-caspase-1 (1:100). To further confirm the presence of the inflammasomes specifically in the podocytes of the mouse glomeruli, NALP3 or caspase-1 was co incubated with a podocin antibody (1:400; Sigma, St. Louis, MO). Double immunofluorescent staining was achieved by incubating with either Alexa-488 or Alexa-555-labeled secondary antibodies for 1 hour at room temperature. After washing, slides were mounted with a DAPI-containing mounting solution, and then observed with a confocal laser

scanning microscope (Fluoview FV1000, Olympus, Japan). As previously described, images were analyzed by the Image Pro Plus 6.0 software (Media Cybernetics, Bethesda, MD), where colocalization was measured and expressed as the Pearson Correlation Coefficient.

Size-exclusion chromatography

Cultured podocytes were treated with or without Hcys and various inhibitors according to the methods mentioned above. Protein was extracted from the homogenized cells with the following protein extraction buffer: 20 mM 4-(2-hydroxyethyl)-1-piperazineethanesulfonic acid-KOH (ph 7.5), 10 mM KCl, 1.5 mM Na-EDTA, 1 mM Na-EGTA, and 1x protease inhibitor cocktail (Roche Applied Science, Indianapolis, IN). Samples were ultracentrifuged at 18,000*g* for 10 minutes at 4 ℃, protein concentration of the supernatant was measured, and 1 mg of protein was run on a Superose 6 10/300 GL Column connected to an ÄKTAprime plus chromatography system (GE Healthscience, Uppsala, Sweden). Fractions (600 µl) were collected starting at the void time and analyzed by western blot. 5x loading buffer was added directly to the samples, heated at 95 ℃ for 5 minutes, run on a SDS-polyacrylamide gel, and transferred to a PVDF membrane. After blocking, the membrane was probed with anti-NALP3 (1:300, Abcam) and anti-ASC (1:1000, Enzo) overnight at 4 ℃, followed by incubation with horseradish peroxidase-labeled IgG (1:3000). The bands were detected by chemiluminescence, visualized on Kodak Omat X-ray films, and band density analyzed by the ImageJ software (NIH, Bethesda, MD).

ASC and gp91^{phox} siRNA transfection

Both ASC and gp91^{phox} siRNA were purchased from Qiagen (Valencia, CA) and confirmed by the company to effectively silence the ASC and gp91^{phox} genes. A nonsilencing, double-stranded

RNA (Qiagen) was used as a negative control. Briefly, podocytes were incubated with serum-free medium for 15 minutes prior to ASC, gp91^{phox}, or scrambled siRNA transfection using the siLentFect Lipid Reagent (Bio-Rad, Hercules, CA) according to the manufacturer's instructions. After 18 hours of incubation at 37℃, the medium was changed, and cells were treated with 40 μM Hcys for 24 hours.

Caspase-1 activity, IL-1β production, and albumin excretion

Caspase-1 activity was measured by a commercially available colorimetric assay kit (Biovision, Mountain View, CA). IL-1β production was measured by a commercially available ELISA kit (R&D System, Minneapolis, MN), according to the manufacturer's instructions. Urinary albumin excretion was also measured using a commercially available mouse albumin ELISA kit (Bethyl Laboratories, Montgomery, TX).

Electromagnetic spin resonance (ESR) analysis of superoxide production

Protein from cultured podocytes was extracted using a sucrose buffer, and then prepared for analysis by resuspension in a modified Krebs-Hepes buffer containing deferoximine (100 μM; Sigma, St. Louis, MO, USA) and diethyldithiocarbamate (5 μM; Sigma). To measure NADPH oxidase-dependent superoxide production, 1 mM NADPH substrate was added to 50 μg protein, and each sample was read twice and examined in the presence or absence of superoxide dismutase (SOD, 200 U/ml; Sigma). 1-hydroxy-3-methoxycarbonyl-2,2,5,5-tetramethylpyrrolidine (CMH, 1mM), a superoxide specific spin trapping compound, was added to the sample before being loaded into a glass capillary, and analyzed in an ESR spectrometer for 10 minutes (1). Results were obtained by taking the difference between the total CMH signal

without SOD and the SOD-specific signal, and all values were expressed as the fold changes of the control.

Indirect immunofluorescent staining

Cells cultured in 8-well chambers were fixed in 4% paraformaldehyde (PFA) for 15 min. After rinsing with phosphate-buffered saline, cells were incubated overnight in 4 ° with rabbit anti-podocin (1:200, Sigma) or mouse anti-desmin (1: 200, BD Pharmingen, San Jose, CA) antibodies. After washing, the slides were incubated with Alexa 488-labeled secondary antibodies for 1 h at room temperature. After being mounted with DAPI-containing mounting solution, the slides were observed under a fluorescence microscope, and photos were taken and analyzed (1). For each chamber, at least 50 cells in 4 nonover lapping fields were counted for podocin and desmin positive cells, and calculated as the percentage of the total number of cells counted.

F-actin staining

To determine the role of NADPH oxidase and inflammasome activation in Hcys-induced cytoskeleton changes, podocytes were cultured in 8-well chambers. After pretreatment with different inhibitors for 30 min, the cells were treated with L-Hcys (40 μM) or puromycin aminonucleoside (PAN, 100 μg/mL, Sigma, St. Louis, MO) for 24 h. After washing with PBS, the cells were fixed in 4% PFA for 15 min at room temperature, permeabilized with 0.1% Triton X-100, and blocked with 3% bovine serum albumin. F-actin was stained with rhodamine–phalloidin (Invitrogen, Carlsbad, CA) for 15 min at room temperature. After mounting, the slides were examined by a confocal laser scanning microscope (Fluoview FV1000, Olympus, Japan).

Cells with distinct F-actin fibers were counted as described previously (4). Scoring was obtained from 100 podocytes on each slide in different groups.

Immunohistochemistry

Kidneys were embedded with paraffin and 5 μm sections were cut from the embedded blocks. After heat-induced antigen retrieval, CD43 staining of T cells and WT-1 staining of podocytes required citrate buffer antigen retrieval, while F4/80 staining of macrophages required Proteinase K antigen retrieval. After a 20 min wash with 3% H_2O_2 and 30 min blocking with serum, slides were incubated with primary antibodies diluted in phosphate-buffered saline (PBS) with 4% serum. Anti-CD43 (1:50; Santa Cruz Biotechnology, Santa Cruz, CA), anti-F4/80 (1:50; AbD Serotec, Raleigh, NC), and anti-WT-1 (1:50; Abcam, Cambridge, MA) antibodies were used in this study. After incubation with each of these primary antibodies overnight, the sections were washed in PBS and incubated with biotinylated IgG (1:200) for 1 h and then with streptavidin-HRP for 30 min at room temperature. 50 μl of DAB was added to each kidney section and stained for 1 min. After washing, the slides were counterstained with hematoxylin for 5 min. The slides were then mounted and observed under a microscope in which photos were taken. All of the glomeruli in the cortical fields were counted and used for analysis in each slide (2).

Glomerular morphological examination

Renal tissues were fixed with a 10% formalin solution, paraffin-embedded, and stained with periodic acid–Schiff (PAS). Renal morphology was observed using a light microscope, and glomerular sclerosis was assessed semiquantitatively and expressed as glomerular damage index (GDI) (3). Fifty glomeruli per slide were counted and scored as 0, 1, 2, 3, or 4, according to 0,

<25, 25–50, 51–75, or >75% sclerotic changes, respectively, across a longitudinal kidney section. The GDI for each mouse was calculated by the formula ((N1 ×1) + (N2 ×2) + (N3 ×3) + (N4 ×4))/n, where N1, N2, N3, and N4 represent the numbers of glomeruli exhibiting grades 1, 2, 3, and 4, respectively, and n is the total number of glomeruli scored.

Co-immunoprecipitation (Co-IP)

Control and Hcys-treated podocytes were scraped in PBS, pelleted by centrifugation, and resuspended in IP lysis buffer (30 mM Tris-HCl, 150 mM NaCl, 2 mM EDTA, 1% Triton X-100, 10% glycerol, 1x Protease Inhibitor). After a 10 minute incubation and aspiration through a 22 gauge needle, the lysate supernatant was precleared by incubation with Protein A/G PLUS-Agarose Beads (Santa Cruz, sc-2003) in 4°. Precleared supernatant was incubated with 2μg antibody against ASC (Enzo, Plymouth Meeting, PA) for 4 hours on a rocker in 4°. Beads were added for an additional 1 hour, immunoprecipitates collected by centrifugation at 1,000g for 5 minutes and then washed three times with IP lysis buffer with centrifugation after each wash. Pellet was resuspended in 2x sample buffer, boiled, and analyzed for NALP3 or caspase-1 protein expression by SDS-PAGE and Western blotting.

Microsome isolation

Podocyte cell lysate was subject to centrifugation at 1000g for 10 minutes at 4° to remove the nuclear fraction. The collected supernatant was then centrifuged at 10000g for 20 minutes at 4° to remove the granular fraction. The resulting supernatant was assayed for protein concentration to normalize protein loading across all samples, and subject to a final centrifugation at 100000g for 90 minutes at 4° to separate the microsomes (pellet) and cytosolic fraction (supernatant). The

isolated pellet was then immediately assayed by electromagnetic spin resonance analysis as described above.

Statistical analysis

All results are expressed as mean ± SEM, and significance was determined by using one-way ANOVA followed by the Tukey-Kramer post hoc test. χ^2 test was used to determine significance of ratio and percentage data. $P<0.05$ was considered statistically significant.

RESULTS

Scrambled gp91*ds-tat* peptide had no effect on hHcys-induced inflammasome formation

We performed additional *in vitro* and *in vivo* experiments using a scrambled gp91*ds-tat* peptide to serve as a control. Confocal microscopic analysis demonstrated that scrambled gp91*ds-tat* peptide did not influence inflammasome formation during either control or Hcys treatment in cultured podocytes (Supplementary Figure S2A). Furthermore, electron spin resonance experiments showed that the scrambled gp91*ds-tat* peptide also did not affect NADPH oxidase-derived $O_2^{\cdot -}$ production in podocytes (Supplementary Figure S2B).

To further confirm the effect of scrambled gp91*ds-tat* peptide *in vivo* in experimental hHcys mice, using confocal microscopy we determined the colocalization of NALP3 with ASC or caspase-1 in glomeruli of hyperhomocysteinemic mice with or without scrambled gp91*ds-tat* peptide treatment. Consistent with *in vitro* studies, scrambled gp91*ds-tat* peptide had no effect on inflammasome formation in control or hyperhomocysteinemic mice (Supplementary Figure S2C).

gp91*ds-tat* peptide administration blocked Hcys-induced loss of podocyte number

To further demonstrate the presence of podocyte injury, we performed immunohistochemical staining of WT-1, a podocyte specific marker, to demonstrate the diminished number of podocytes within the glomeruli of hyperhomocysteinemic mice. It was found that hHcys induced a significant decrease in podocyte number compared to control mice and this effect was substantially blocked in those receiving the gp91*ds-tat* peptide (Supplementary Figure S3).

REFERENCES

1. Boini KM, Xia M, Li C, Zhang C, Payne LP, Abais JM, Poklis JL, Hylemon PB, Li PL. Acid sphingomyelinase gene deficiency ameliorates the hyperhomocysteinemia-induced glomerular injury in mice. *Am J Pathol* 179: 2210-9, 2011.
2. De Miguel C, Guo C, Lund H, Feng D, Mattson DL. Infiltrating T lymphocytes in the kidney increase oxidative stress and participate in the development of hypertension and renal disease. *Am J Physiol Renal Physiol* 300: F734-42, 2011.
3. Raij L, Azar S, Keane W. Mesangial immune injury, hypertension, and progressive glomerular damage in Dahl rats. *Kidney Int* 26: 137-43, 1984.
4. Yang L, Zheng S, Epstein PN. Metallothionein over-expression in podocytes reduces adriamycin nephrotoxicity. *Free Radic Res* 43: 174-82, 2009.
5. Zhang C, Boini KM, Xia M, Abais JM, Li X, Liu Q, Li PL. Activation of Nod-like receptor protein 3 inflammasomes turns on podocyte injury and glomerular sclerosis in hyperhomocysteinemia. *Hypertension* 60: 154-62, 2012.

FIGURE LEGENDS

Figure S1. NADPH oxidase inhibition attenuated Hcys-induced immunoprecipitation of inflammasome proteins. A. Immunoprecipitation and Western blot analysis of the interaction of NALP3 and caspase-1 with ASC in lysates of Hcys-treated podocytes. B and C. Summarized data of the Western blot intensities of NALP3-coimmunoprecipitated with ASC (B) and caspase-1-coimmunoprecipitated with ASC (C) (n=5). * P<0.05 vs. Control; # P<0.05 vs. Hcys.

Figure S2. Scrambled gp91*ds-tat* peptide had no effect on hHcys-induced inflammasome formation *in vitro* and *in vivo*. A. Colocalization of NALP3 (green) with ASC (red) and NALP3 (green) with caspase-1 (red) in cultured podocytes (n=4). B. Scrambled gp91*ds-tat* peptide did not influence NADPH oxidase-derived $O_2^{\cdot-}$ production in either control or Hcys-treated podocytes (n=3). C. Scrambled gp91*ds-tat* peptide did not affect hHcys-induced inflammasome formation and colocalization between NALP3 (green) with ASC (red) and NALP3 (green) with caspase-1 (red) in glomeruli of mice (n=3). Ctrl: Control; Vehl: Vehicle; Scrm*ds-tat*: Scrambled gp91*ds-tat* peptide. * P<0.05 vs. Control; # P<0.05 vs. Hcys.

Figure S3. Amelioration of Hcys-induced podocyte injury by inhibition of NADPH oxidase expression and activity in mice fed a FF diet. Colocalization of NALP3 (green) with podocyte marker, desmin (red) and caspase-1 (green) with desmin (red) in the mouse glomeruli of gp91$^{phox+/+}$, gp91*ds-tat*, and gp91$^{phox-/-}$ mice fed a normal or FF diet (n=4).

Figure S4. Attenuation of podocyte loss in the glomeruli of gp91*ds-tat* peptide-treated mice. A. Representative images of WT-1-stained glomeruli in control and gp91*ds-tat* peptide mice on

either normal or FF diet (Original magnification, x400). B. Summarized data showing podocyte numbers per glomerulus in each group (n=4-5). * $P<0.05$ vs. $gp91^{phox+/+}$ on Normal Diet; # $P<0.05$ vs. $gp91^{phox+/+}$ on FF Diet.

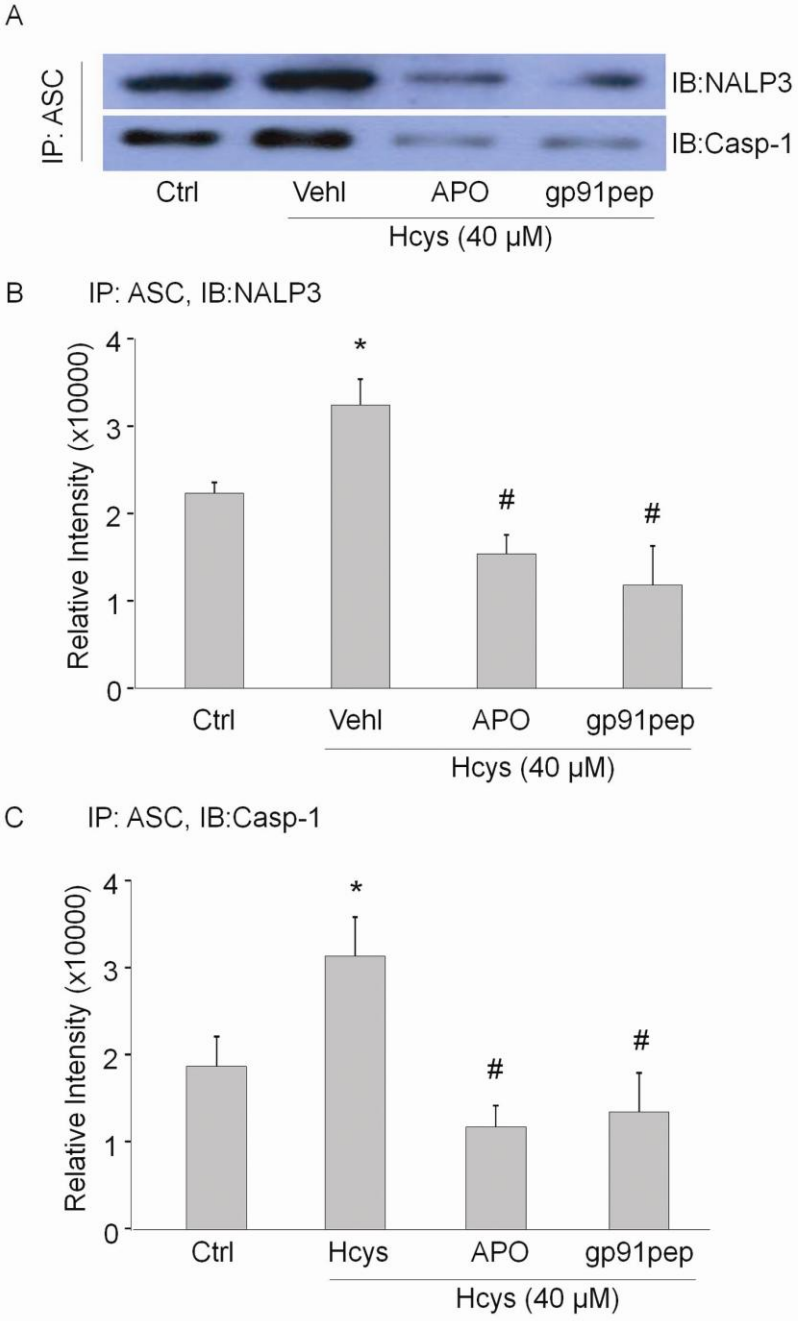

Figure S1

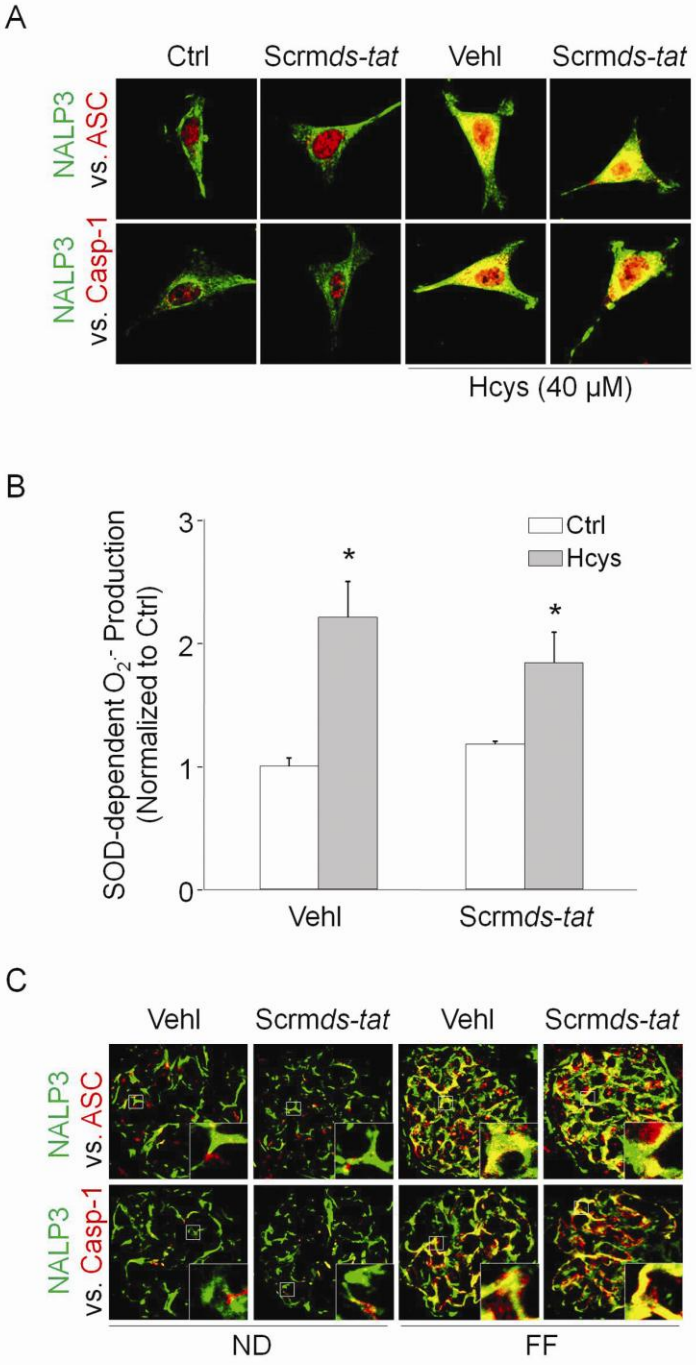

Figure S2

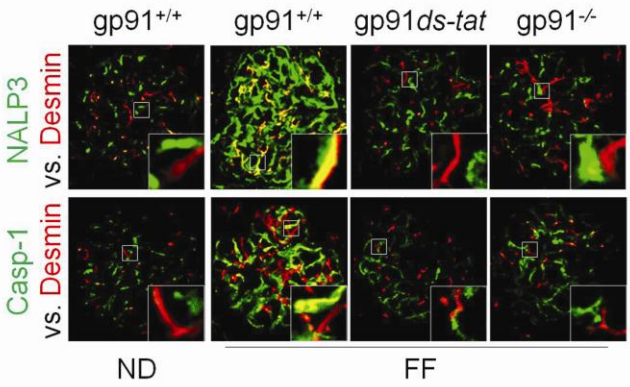

Figure S3

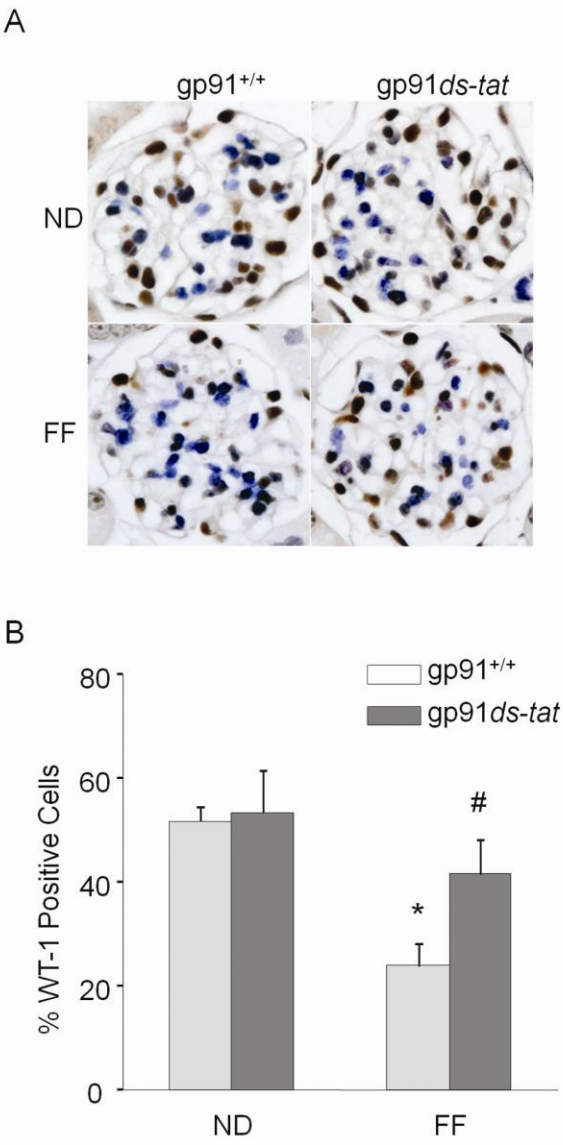

Figure S4